4.3. Immunohistochemistry

Immunostaining of cultured hippocampal slices was performed according to the method of Qin et al. (2001) with modifications. Slices were fixed with ice-cold 4% (wt/vol) PFA in 0.1 M phosphate buffer (PB) for 10 min at 4 °C, washed with phosphate buffered saline (PBS) (5 min×3), and treated with 1% (vol/vol) Triton X-100 in PBS overnight at 4 °C. Slices were then blocked with 50 mM ammonium chloride for 30 min at 4 °C and 20% HS in PBS for 30 min at 4 °C. Subsequent steps were carried out using PBS containing 1% HS. Slices were treated with mouse monoclonal IgG to PSD95 (1:1000) overnight at 4 °C, washed (15 min×3), and treated with Alexa Fluor 488 rabbit anti-mouse IgG (1:1000) overnight at 4 °C. After washing (15 min×3), fluorescent images were obtained by confocal microscopy (BioRad μ-Radiance laser scanning confocal system) using a 4×objective. Black level was set so that the averaged fluorescence intensity of 5 independent squares (20 μm×20 μm) placed at the medial position of CA1 stratum pyramidale (SP) of the control slice had the same value as that of the outside of the slice. Gain level was set so that the averaged fluorescence intensity of 5 squares (20 μm×20 μm) placed at the medial position of CA3SL of the control slice was at the half-maximum level. In gray-scale mode under these settings, the major synaptic sites appeared as fluorescent compartments as shown in Fig. 1B. When we outlined these compartments as indicated in Fig. 1B and calculated the areas, the values were constant regardless of the treatment (data not shown), so, we measured the averaged fluorescence intensity of each compartment (an outlined area) and subtracted the back ground intensity to quantify the expression level of PSD95 of each synaptic site. Because slices were cultured after removing entorhinal cortex, we quantified the expression of PSD95 in CA1SR, CA1SO, CA3SL, and CA3SO, the synaptic sites which maintain the intact presynaptic and postsynaptic cells (Fig. 1B).

4.4. DiI staining

Cultured hippocampal slices were fixed with 4% PFA for 30 min at 4 °C. The fixative above the transmembrane was removed and DiI crystals were embedded into CA1SO and CA3SO under the light microscope. After 3 days of incubation at 4 °C, fluorescent images were obtained by confocal microscopy using a 60×objective. Horizontal optical sections were taken at 0.5 μm steps and the resultant z-series images were summed into a flat image. Spines (both dendritic filopodia and mature spines) were counted at the proximal sites of apical dendrites projecting from pyramidal cell bodies. For double labeling with DiI and PSD95 immunostaining, slices were immunostained after 3 days of incubation with DiI crystals.

4.5. Fluorescent Nissl staining

Cultured hippocampal slices were fixed with 4% PFA for 60 min at 4 °C. Subsequent steps were carried out at room temperature. After washing with PBS (15 min×3), the slices were treated with 0.1% Triton X-100 in PBS for 60 min, washed with PBS for 10 min, and incubated with NeuroTrace fluorescent Nissl (1:30 in PBS) for 40 min in a dark room. The incubation was terminated by a 10 min wash with 0.1% Triton X-100 in PBS, followed by 2 h wash with PBS. Fluorescent images were obtained by confocal microscopy using a 60×objective.

4.6. Subregional hippocampal neuron culture

Subregional neuron cultures of both genders of P3 Wistar rat hippocampi were prepared according to the method of Ikegaya et al. (2000). Ammon's horn and DG were isolated from hippocampi with extreme care so as not to mix these 2 regions (Fig. 4A, right). Dissociated cells from Ammon's horn, DG, or a combination of these regions were suspended in a 1:1 mixture of astrocyte-conditioned medium (ACM) and NB/B27 medium (2% [v/v] B-27 supplement and 73 μg/ml L-glutamine in NB) and plated onto 48-well plates coated with poly-L-lysine. After 24 h, the medium was changed to ACM-free NB/B-27 medium containing 2 μM AraC. Cells derived from each region were cultured for 7 days at the same cell density (2×10^4 cells/cm^2 for FM1-43 analysis, 5×10^5 cells/cm^2 for Western blot analysis and ELISA detection of BDNF). All surviving cells were immunohistochemically confirmed to be neurons using anti-NeuN antibody (data not shown).

4.7. FM1-43 analysis

After 1 h of incubation with HBSS at 37 °C, cultured neurons were treated with 10 μM FM1-43, a styryl pyridinium dye (Cochilla et al., 1999) in high K$^+$-HBSS (20 mM KCl; osmolarity maintained by concomitant decrease in sodium concentration) for 2 min and washed gently with HBSS for 1 min. To reduce background staining, neurons were washed with 20 μM ADVASEP-7, a sulphobutylated derivative of β-cyclodextrin (Tait et al., 1992) for 1 min. ADVASEP-7 has a higher affinity for FM1-43 than plasma membranes and has been shown to greatly reduce background staining in brain slices (Kay et al., 1999). After the incubation with 10 μM TTX for 30 min, three images ([1] stained image; [2] destained image obtained after the treatment with high K$^+$-HBSS; and [3] differential interference contrast [DIC] image) were obtained for each microscopic field of view using confocal microscopy with a 10× objective. The second image was subtracted from the first, which revealed the presynaptic sites where depolarization-specific release had occurred (Fig. 4C, top panels). The fluorescent puncta in each microscopic field of view were counted. The number of synapses per neuron was estimated by dividing the total number of puncta by the number of neurons observed in the third (DIC) image (Fig. 4C, bottom panels).

4.8. Western blot analysis

Cultured neurons were washed twice with ice-cold PBS and then harvested on ice with 50 mM Tris buffer (pH 7.2) containing 1 mM EDTA, 1 mM phenylmethylsulphonyl fluoride, 1 mM leupeptin, 1 μg/ml antipain and 1 μg/ml aprotinin. After intense sonication (23 kHz, 1 min×3), the cell suspension was centrifuged at 800×g for 5 min at 4 °C. An

aliquot of this supernatant was removed for the protein assay. Another aliquot was diluted in SDS sample buffer. Protein samples containing an equal amount of protein were separated by electrophoresis on 10% polyacrylamide-SDS gels and transferred onto polyvinyliden difluoride membranes in 49.6 mM Tris, 384 mM glycine and 0.01% (wt/vol) SDS at 30 V overnight followed by 80 V for 1 h. The membranes were incubated with Tris-buffered saline (TBS) containing 0.1% (vol/vol) Tween 20, 5% (wt/vol) skim milk, 2% (wt/vol) BSA, and 0.1% (wt/vol) sodium azide for 1 h, followed by overnight incubation with protein A purified rabbit anti-BDNF polyclonal antibody (AB1534SP, Chemicon) (1:1000) or rabbit polyclonal IgG to β-actin (1:1000) at 4 °C. After washing (30 min), the membranes were then incubated with peroxidase-conjugated anti-rabbit IgG (1:1000) for 1 h at room temperature. Immunoreactive bands were visualized using the ECL kit. Optical densities (ODs) of immunoreactive bands were measured based on a gray scale of 0–256 arbitrary units. Background was subtracted from the OD and this corrected value was normalized to the corrected value of the β-actin band obtained from the same sample.

4.9. ELISA detection of BDNF

In comparison of BDNF contents in cultured DG neurons and cultured Ammon's horn neurons, cells were washed twice with ice-cold PBS and then harvested on ice with homogenization buffer consisting of 100 mM Trin/HCl (pH7), containing 2% (wt/vol) BSA, 1 M NaCl, 4 mM EDTA.Na2, 2% (vol/vol) Triton X-100, 0.1% (wt/vol) sodium azide, 5 μg/ml aprotinin, 0.5 μg/ml antipain, 157 μg/ml benzamidine, 0.1 μg/ml pepstatin A and 17 μg/ml phenylmethyl–sulphonyl fluoride. After intense sonication (23 kHz, 1 min×3), the homogenates are centrifuged at 14,000×g for 30 min. An aliquot of this supernatant was removed for the protein assay. Another aliquot was subjected to the calculation of BDNF concentration by the Chemikine BDNF sandwich ELISA kit. The plates, which were pre-coated with monoclonal antibodies against BDNF, were incubated with 100 μl of supernatant in each well overnight, followed by incubation with the secondary antibody for 3 h and color developing procedures for 1 h. Immediately after the stop solution included in the kit was added, the ODs of 450 nm were measured. A standard curve was run for each plate and linearity was confirmed for all detections. Because the lower detection limit of the kit is 7.8 pg/ml, we used data from the experiments in which the control value was higher than this limit. The concentration of BDNF was normalized to the total amount of protein. In the calculation of BDNF contents in the culture media, the culture media were collected after 10 h of incubation with E2, centrifuged at 1500×g, and the concentration of BDNF in the supernatants was determined by ELISA. Because in this case the values of the control group varied from experiment to experiment by several folds, we set 'basal value' in each experiment. 24 h after medium change, BDNF concentrations in the culture media were calculated and averaged for 4 wells in one experiment. This value was taken as the 'basal value' and the data were normalized to this 'basal value' in each experiment.

4.10. Drug treatment

E2 was dissolved at 100 mM in ethanol and diluted to the final concentrations with the culture medium. For PSD95 immunohistochemistry and FM1-43 analysis, cultured slices and cells were treated with various concentrations of E2 for 24 h. ICI (Ki: 1.5 nM for ERα, 6.4 nM for ERβ; Kuiper et al., 1997) was dissolved at 1 mM in ethanol and co-applied at 1 μM with E2. K252a (Squinto et al., 1991; Bothwell, 1995) was dissolved at 1 mM in DMSO and co-applied at 200 nM with E2. This concentration completely blocks the effect of BDNF in cultured hippocampal slices (Koyama et al., 2004). BDNFAB (protein A purified sheep anti-BDNF polyclonal antibody, AB1513SP, Chemicon) was dissolved in the culture medium at 10 μg/ml. This concentration blocks the effect of endogenous BDNF (Rasika et al., 1999; Matsunaga et al., 2004). For ELISA detection of the released BDNF, cultured cells were treated with E2 for 10 h. KT5720 (Ki: 56 nM) (Kase et al., 1987) was dissolved in the ethanol at 1 mM and co-applied at 200 nM with E2. Rp-cAMP (Ki: 11 μM) (Rothermel and Parker Botelho, 1988) was dissolved in PBS at 10 mM and co-applied at 10 μM with E2. U0126 (Ki: 72 nM for MEK1, 58 nM for MEK2) (Duncia et al., 1998) was dissolved in DMSO at 10 mM and co-applied at 10 μM with E2. We also confirmed beforehand that 0.1% ethanol or 0.1% DMSO (the maximal concentration used for vehicle in our experiments) alone had no effects in cultured hippocampal slices and subregional hippocampal neuron cultures (Fig. S1).

4.11. Data analysis

All data regarding the expression level of PSD95, the spine density, and the number of FM1-43 positive puncta, were quantified in a blinded manner. For quantification of PSD-95 signals, the fluorescence intensities in the synaptic sites were averaged for 4 slices in one experiment. These values were then averaged for 8 independent experiments (separate platings) and statistical analysis was performed using oneway repeated-measure analysis of variance (ANOVA) and the post hoc Tukey's test for multiple pairwise comparisons. Data are shown as the values normalized to that of CA1SR in the control group. The spine densities (the number of spines per μm of dendrite) averaged for 8 to 10 neurons per slice were averaged for 4 slices in 1 experiment. These values were then averaged for 8 independent experiments (separate platings) and statistical analysis was performed using the Student's t test. For FM1-43 analysis, the numbers of presynaptic sites (per neuron) were averaged for 4 wells in 1 experiment. These values were then averaged for 8 independent experiments (separate platings) and statistical analysis was performed using the Student's t test. In multiple pharmacological treatments, data were collected according to the methods described above, and statistical analysis was performed by one-way repeated-measure ANOVA and the post hoc Tukey's test for multiple pairwise comparisons. Data were shown as the values normalized to that of the control group. For ELISA detection of BDNF expression, the normalized values (BDNF/total protein) were averaged for 4 wells in one experiment. These values were then averaged for 4 independent experiments (separate platings) and statistical analysis was

performed by one-way repeated-measure ANOVA and the post hoc Tukey's test for multiple pairwise comparisons. For ELISA detection of the released BDNF, the values normalized to the basal value were averaged for 4 wells in one experiment. These values were then averaged for 4 independent experiments (separate platings) and statistical analysis was performed using one-way repeated-measure ANOVA and the post-hoc Tukey's test for multiple pairwise comparisons. Values of $p < 0.05$ were considered significant.

Acknowledgments

Appendix A. Supplementary data

Supplementary data associated with this article can be found, in the online version, at doi:10.1016/j.brainres.2007.02.093.
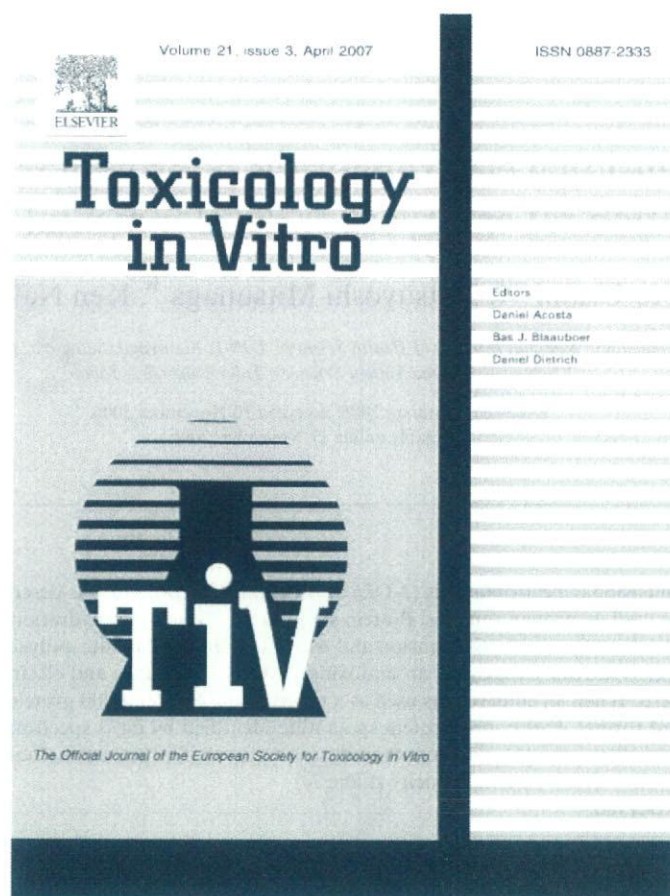
REFERENCES

Acsady, L., Kamondi, A., Sik, A., Freund, T., Buzsaki, G., 1998. GABAergic cells are the major postsynaptic targets of mossy fibers in the rat hippocampus. J. Neurosci. 18, 3386–3403.

Aguado, F., Carmona, M.A., Pozas, E., Aguilo, A., Martinez-Guijarro, F.G., Alcantara, S., Borrell, V., Yuste, R., Ibanez, C.F., Soriano, E., 2003. BDNF regulates spontaneous correlated activity at early developmental stages by increasing synaptogenesis and expression of the K+/Cl– co-transporter KCC2. Development 130, 1267–1280.

Alsina, B., Vu, T., Cohen-Cory, S., 2001. Visualizing synapse formation in arborizing optic axons in vivo: dynamics and modulation by BDNF. Nat. Neurosci. 4, 1093–1101.

Balkowiec, A., Katz, D.M., 2002. Cellular mechanisms regulating activity-dependent release of native brain-derived neurotrophic factor from hippocampal neurons. J. Neurosci. 22, 10399–10407.

Beyer, C., Karolczak, M., 2000. Estrogenic stimulation of neurite growth in midbrain dopaminergic neurons depends on cAMP/protein kinase A signaling. J. Neurosci. Res. 59, 107–116.

Beyer, C., Ivanova, T., Karolczak, M., Kuppers, E., 2002. Cell type-specificity of nonclassical estrogen signaling in the developing midbrain. J. Steroid Biochem. Mol. Biol. 81, 319–325.

Beyer, C., Pawlak, J., Karolczak, M., 2003. Membrane receptors for oestrogen in the brain. J. Neurochem. 87, 545–550.

Bothwell, M., 1995. Functional interactions of neurotrophins and neurotrophins receptors. Annu. Rev. Neurosci. 18, 223–253.

Cambiasso, M.J., Carrer, H.F., 2001. Nongenomic mechanism mediates estradiol stimulation of axon growth in male rat hypothalamic neurons in vitro. J. Neurosci. Res. 66, 475–481.

Clarke, C.H., Norfleet, A.M., Clarke, M.S., Watson, C.S., 2000. Perimembrane localization of the estrogen receptor (protein in neuronal processes of cultured hippocampal neurons. Neuroendocrinology 71, 34–42.

Cochilla, A.J., Angleson, J.K., Betz, W.J., 1999. Monitoring secretory membrane with FM1-43 fluorescence. Ann. Rev. Neurosci. 22, 1–10.

Craven, S.D., Bredt, D.S., 1998. PDZ proteins organize synaptic signaling pathways. Cell 93, 495–509.

Danzer, S.C., McNamara, J.O., 2004. Localization of brain-derived neurotrophic factor to distinct terminals of mossy fiber axons implies regulation of both excitation and feedforward inhibition of CA3 pyramidal cells. J. Neurosci. 24, 11346–11355.

De Simoni, A., Griesinger, C.B., Edwards, F.A., 2003. Development of rat CA1 neurones in acute versus organotypic slices: role of experience in synaptic morphology and activity. J. Physiol. 550 (Pt. 1), 135–147.

Dieni, S., Rees, S., 2002. Distribution of brain-derived neurotrophic factor and TrkB receptor proteins in the fetal and postnatal hippocampus and cerebellum of the guinea pig. J. Comp. Neurol. 454, 229–240.

Duncia, J.V., Santella III, J.B., Higley, C.A., Pitts, W.J., Wityak, J., Frietze, W.E., Rankin, F.W., Sun, J.H., Earl, R.A., Tabaka, A.C., Teleha, C.A., Blom, K.F., Favata, M.F., Manos, E.J., Daulerio, A.J., Stradley, D.A., Horiuchi, K., Copeland, R.A., Scherle, P.A., Trzaskos, J.M., Magolda, R.L., Trainor, G.L., Wexler, R.R., Hobbs, F.W., Olson, R.E., 1998. MEK inhibitors: the chemistry and biological activity of U0126, its analogs, and cyclization products. Bioorg. Med. Chem. Lett. 8 (20), 2839–2844.

Garner, C.C., Nash, J., Huganir, R.L., 2000. PDZ domains in synapse assembly and signaling. Trends Cell Biol. 10, 274–280.

Gartner, A., Staiger, V., 2002. Neurotrophin secretion from hippocampal neurons evoked by long-term-potentiation-inducing electrical stimulation patterns. Proc. Natl. Acad. Sci. U. S. A. 99 (9), 6386–6391.

Germain, S.J., Campbell, P.S., Anderson, J.N., 1978. Role of the serum estrogen-binding protein in the control of tissue estradiol levels during postnatal development of the female rat. Endocrinology 103, 1401–1410.

Gould, E., Woolley, C.S., Frankfurt, M., McEwen, B.S., 1990. Gonadal steroids regulate dendritic spine density in hippocampal pyramidal cells in adulthood. J. Neurosci. 10, 1286–1291.

Hartmann, M., Heumann, R., Lessmann, V., 2001. Synaptic secretion of BDNF after high frequency stimulation of glutamatergic synapses. EMBO J. 20, 5887–5897.

Haubensak, W., Narz, F., Heumann, R., Lessmann, V., 1998. BDNF-GFP containing secretory granules are localized in the vicinity of synaptic junctions of cultured cortical neurons. J. Cell Sci. 111, 1483–1493.

Hojo, Y., Hattori, T., Enami, T.A., Hurukawa, A., Suzuki, K., Ishii, H.T., Mukai, H., Morrison, J.H., Janssen, W.G., Kominami, S., Harada, N., Kimoto, T., Kawato, S., 2004. Adult male rat hippocampus synthesizes estradiol from pregnenolone by cytochromes P45017α and P450 aromatase localized in neurons. Proc. Natl. Acad. Sci. U. S. A. 101, 865–870.

Ikegaya, Y., Nishiyama, N., Matsuki, N., 2000. L-type Ca^{2+} channel blocker inhibits mossy fiber sprouting and cognitive deficits following pilocarpine seizures in immature mice. Neuroscience 98, 647–659.

Ivanova, T., Kuppers, E., Engele, J., Beyer, C., 2001. Estrogen stimulates brain-derived neurotrophic factor expression in embryonic mouse midbrain neurons through a membrane-mediated and calcium-dependent mechanism. J. Neurosci. Res. 66, 221–230.

Jontes, J.D., Smith, S.J., 2000. Filopodia, spines, and the generation of synaptic diversity. Neuron 27, 11–14.

Kase, H., Iwahashi, K., Nakanishi, S., Matsuda, Y., Yamada, K., Takahashi, M., Murakata, C., Sato, A., Kaneko, M., 1987. K-252 compounds, novel and potent inhibitors of protein kinase C

and cyclic nucleotide-dependent protein kinases. Biochem. Biophys. Res. Commun. 142, 436–440.

Kay, A.R., Alfonso, A., Alford, S., Cline, H.T., Holgado, A.M., Sakmann, B., Snitsarev, V.A., Stricker, T.P., Takahashi, M., Wu, L.G., 1999. Imaging synaptic activity in intact brain and slices with FM1-43 in C. elegans, lamprey, and rat. Neuron 24, 809–817.

Kelly, M.J., Levin, E.R., 2001. Rapid actions of plasma membrane estrogen receptors. Trends Endocrinol. Metab. 12, 152–156.

Koyama, R., Yamada, M.K., Fujisawa, S., Katoh-Semba, R., Matsuki, N., Ikegaya, Y., 2004. Brain-derived neurotrophic factor induces hyperexcitable reentrant circuits in the dentate gyrus. J. Neurosci. 24, 7215–7224.

Kramar, E.A., Lin, B., Lin, C.Y., Arai, A.C., Gall, C.M., Lynch, G., 2004. A novel mechanism for the facilitation of theta-induced long-term potentiation by brain-derived neurotrophic factor. J. Neurosci. 24 (22), 5151–5161.

Kretz, O., Fester, L., Wehrenberg, U., Zhou, L., Brauckmann, S., Zhao, S., Prange-Kiel, J., Naumann, T., Jarry, H., Frotscher, M., Rune, G.M., 2004. Hippocampal synapses depend on hippocampal estrogen synthesis. J. Neurosci. 24, 5913–5921.

Kuiper, G.G., Carlsson, B., Grandien, K., Enmark, E., Haggblad, J., Nilsson, S., Gustafsson, J.A., 1997. Comparison of the ligand binding specificity and transcript tissue distribution of estrogen receptors alpha and beta. Endocrinology 138, 863–870.

Lawrence, J.J., McBain, C.J., 2003. Interneuron diversity series: containing the detonation-feedforward inhibition in the CA3 hippocampus. Trends Neurosci. 26, 631–640.

Lessmann, V., Gottmann, K., Malcangio, M., 2003. Neurotrophin secretion: current facts and future prospects. Prog. Neurobiol. 69, 341–374.

Matsunaga, W., Shirokawa, T., Isobe, S., 2004. BDNF is necessary for maintenance of noradrenergic innervations in the aged rat brain. Neurobiol. Aging 25, 341–348.

McAllister, A.K., Katz, L.C., Lo, D.C., 1999. Neurotrophins and synaptic plasticity. Annu. Rev. Neurosci. 22, 295–318.

McEwen, B., Akama, K., Alves, S., Brake, W.G., Bulloch, K., Lee, S., Li, C., Yuen, G., Milner, T.A., 2001. Tracking the estrogen receptor in neuron: implication for estrogen-induced synapse formation. Proc. Natl. Acad. Sci. U. S. A. 98, 7093–7100.

Mizuhashi, S., Nishiyama, N., Matsuki, N., Ikegaya, Y., 2001. Cyclic nucleotide-mediated regulation of hippocampal mossy fiber development: a target-specific guidance. J. Neurosci. 15 21 (16), 6181–6194.

Murphy, D.D., Cole, N.B., Greenberger, V., Segal, M., 1998a. Estradiol increases dendritic spine density by reducing GABA neurotransmission in hippocampal neurons. J. Neurosci. 18 (7), 2550–2559.

Murphy, D.D., Cole, N.B., Segal, M., 1998b. Brain-derived neurotrophic factor mediates estradiol-induced dendritic spine formation in hippocampal neurons. Proc. Natl. Acad. Sci. U. S. A. 95 (19), 11412–11417.

Nakagami, Y., Saito, H., Matsuki, N., 1997. The regional vulnerability to blockade of action potentials in organotypic hippocampal culture. Brain Res. Dev. Brain Res. 103 (1), 99–102.

Okabe, S., Miwa, A., Okado, H., 2001. Spine formation and correlated assembly of presynaptic and postsynaptic molecules. J. Neurosci. 21, 6105–6114.

Patterson, S.L., Pittenger, C., Morozov, A., Martin, K.C., Scanlin, H., Drake, C., Kandel, E.R., 2001. Some forms of cAMP-mediated long-lasting potentiation are associated with release of BDNF and nuclear translocation of phospho-MAP kinase. Neuron 32, 123–140.

Pozzo-Miller, L.D., Inoue, T., Murphy, D.D., 1999. Estradiol increases spine density and NMDA-dependent Ca^{2+} transients in spines of CA1 pyramidal neurons from hippocampal slices. J. Neurophysiol. 81, 1404–1411.

Qin, L., Marrs, G.S., Mckim, R., Dailey, M.E., 2001. Hippocampal mossy fibers induce assembly and clustering of

PSD95-containing postsynaptic densities independent of glutamate receptor activation. J. Comp. Neurol. 440, 284–298.

Rasika, S., Alvarez-Buylla, A., Nottebohm, F., 1999. BDNF mediates the effects of testosterone on the survival of new neurons in an adult brain. Neuron 22, 53–62.

Razandi, M., Pedram, A., Merchenthaler, I., Greene, G.L., Levin, E.R., 2004. Plasma membrane estrogen receptors exist and functions as dimmers. Mol. Endocrinol. 18, 2854–2865.

Rothermel, J.D., Parker Botelho, L.H., 1988. A mechanistic and kinetic analysis of the interactions of the diastereoisomers of adenosine 3′,5′-(cyclic)phosphorothioate with purified cyclic AMP-dependent protein kinase. Biochem. J. 251, 757A–762A.

Sato, K., Matsuki, N., Ohno, Y., Nakazawa, K., 2002. Effects of 17β-estradiol and xenoestrogens on the neuronal survival in an organotypic hippocampal culture. Neuroendocrinology 76, 223–234.

Scharfman, H.E., MacLusky, N.J., 2005. Similarities between actions of estrogen and BDNF in the hippocampus: coincidence or clue? Trends Neurosci. 28 (2), 79–85.

Scharfman, H.E., Mercurio, T.C., Goodman, J.H., Wilson, M.A., MacLusky, N.J., 2003. Hippocampal excitability increases during the estrous cycle in the rat: a potential role for brain-derived neurotrophic factor. J. Neurosci. 23, 11641–11652.

Segal, M., Murphy, D., 2001. Estradiol induces formation of dendritic spines in hippocampal neurons: functional correlates. Horm. Behav. 40 (2), 156–159.

Segars, J.H., Driggers, P.H., 2002. Estrogen action and cytoplasmic signaling cascades. Part I: membrane-associated signaling complexes. Trends Endocrinol. Metab. 13, 349–354.

Seil, F.J., Drake-Baumann, R., 2000. TrkB receptor ligands promote activity-dependent inhibitory synaptogenesis. J. Neurosci. 20, 5367–5373.

Sohrabji, F., Miranda, R.C., Toran-Allerand, C.D., 1995. Identification of a putative estrogen response element in the gene encoding brain-derived neurotrophic factor. Proc. Natl. Acad. Sci. U. S. A. 92, 11110–11114.

Squinto, S.P., Stitt, T.N., Aldrich, T.H., Davis, S., Bianco, S.M., Radziejewski, C., Glass, D.J., Masiakowski, P., Furth, M.E., Valenzuela, D.M., Distefano, P.S., Yancopolous, G.D., 1991. trkB encodes a functional receptor for brain-derived neurotrophic factor and neurotrophin-3 but not nerve growth factor. Cell 65, 885–893.

Tait, R.J., Skanchy, D.J., Thompson, D.P., Chetwyn, N.C., Dunshee, D.A., Rajewski, R.A., Stella, V.J., Stobaugh, J.F., 1992. Characterization of sulfoalkyl ether derivatives of beta-cyclodextrin by capillary electrophoresis with indirect UV detection. J. Pharm. Biomed. Anal. 10, 615–622.

Takahashi, H., Sekino, Y., Tanaka, S., Mizui, T., Kishi, S., Shirao, T., 2003. Drebrin-dependent actin clustering in dendritic filopodia governs synaptic targeting of postsynaptic density-95 and dendritic spine morphogenesis. J. Neurosci. 23, 6586–6595.

Tanapat, P., Hastings, N.B., Reeves, A.J., Gould, E., 1999. Estrogen stimulates a transient increase in the number of new neurons in the dentate gyrus of the adult female rat. J. Neurosci. 19 (14), 5792–5801.

Thomas, P., Pang, Y., Filardo, E.J., Dong, J., 2004. Identity of an estrogen membrane receptor coupled to a G-protein in human breast cancer cells. Endocrinology 146, 624–632.

Toran-Allerand, C.D., Guan, X., MacLusky, N.J., Horvath, T.L., Diano, S., Singh, M., Connolly Jr., E.S., Nethrapalli, I.S., Tinnikov, A.A., 2002. ER-X: a novel, plasma membrane-associated, putative estrogen receptor that is regulated during development and after ischemic brain injury. J. Neurosci. 22, 8391–8401.

Tyler, W.J., Alonso, M., Bramham, C.R., Pozzo-Miller, L.D., 2002. From acquisition to consolidation: on the role of brain-derived neurotrophic factor signaling in hippocampal-dependent learning. Learn. Mem. 9 (5), 224–237.

Woolley, C.S., 1998. Estrogen-mediated structural and functional

synaptic plasticity in the female rat hippocampus. Horm. Behav. 34 (2), 140–148.

Woolley, C.S., Schwartzkroin, P.A., 1998. Hormonal effects on the brain. Epilepsia 39 (Suppl. 8), S2–S8.

Wu, Y.J., Kruttgen, A., Moller, J.C., Shine, D., Chan, J.R., Shooter, E.M., Cosgaya, J.M., 2004. Nerve growth factor, brain-derived neurotrophic factor, and neurotrophin-3 are sorted to dense-core vesicles and released via the regulated pathway in primary rat cortical neurons. J. Neurosci. Res. 75, 825–834.

Znamensky, V., Akama, K.T., McEwen, B., Milner, T., 2003. Estrogen levels regulate the subcellular distribution of phosphorylated Akt in hippocampal CA1 dendrites. J. Neurosci. 23, 2340–2347.

Two-dimensional electrophoresis of protein from cultured postimplantation rat embryos for developmental toxicity studies

Makoto Usami [a,*], Katsuyoshi Mitsunaga [b], Ken Nakazawa [a]

[a] *Division of Pharmacology, National Institute of Health Sciences, 1-18-1, Kamiyoga, Setagaya, Tokyo 158-8501, Japan*
[b] *School of Pharmaceutical Sciences, Toho University, Japan*

Abstract

A simple method for two-dimensional electrophoresis (2-DE) of rat embryonic protein was described. Rat embryos cultured for 24 h from day 10.5 of gestation were used as protein samples. Protein samples were lysed in rehydration buffer and separated by isoelectric focusing with immobilized pH gradient for the first dimension and by sodium dodecyl sulfate–polyacrylamide gel electrophoresis for the second dimension. The use of the DeStreak Reagent as an antioxidant in the lysis buffer and electrode pads in the isoelectric focusing greatly improved the 2-DE pattern. When an embryo was used as a protein sample, about 800 protein spots were detected by silver staining in a 2-DE gel of the standard format. Eighty-one protein spots were identified by mass spectrometry for a primary 2-DE map. The same method could be applied to yolk sac membranes from the cultured embryos. The present method was considered to be suitable for a concomitant 2-DE analysis in in vitro developmental toxicity studies.
© 2006 Elsevier Ltd. All rights reserved.

Keywords: Two-dimensional electrophoresis; Rat; Embryo; Yolk sac; Developmental toxicity; Proteome

1. Introduction

Recent advances in two-dimensional electrophoresis (2-DE) made it possible to analyze the changes in protein expression pattern caused by exogenous stimulations in various tissues, such as the liver (Fountoulakis et al., 2000), kidney (Xu et al., 2005) and blood components (Piubelli et al., 2005). In developmental toxicity studies, the analysis of embryonic protein expression pattern by 2-DE is considered to be useful for the mechanism-based evaluation of developmental toxicants.

On the other hand, it is expected that the cultured rat embryos can be better protein samples for the analysis of protein expression pattern in developmental toxicity studies. Postimplantation rat embryo culture is now widely used in developmental toxicity studies, by which embryos can be exposed to test chemicals under controlled conditions with a small number of animals and a small amount of test chemicals (Schmid et al., 1997).

However, there have been no suitable 2-DE methods for the analysis of embryonic protein expression pattern since most methods are for radio-labeled proteins but not for total proteins (Baumgartner et al., 1994; Praxmayer et al., 1992). The standard 2-DE methods that we tried could not be applicable because of a high salt concentration and poor solubility of embryonic samples. A method reported for the proteome analysis of mouse embryos is not considered suitable for routine analysis in developmental toxicity studies because of troublesome pretreatment of embryo samples, i.e., water-wash and dry-ice freezing (Greene et al., 2002).

In the present study, we described a simple 2-DE method for the analysis of cultured postimplantation rat embryos. By our method about 800 protein spots were detected in a
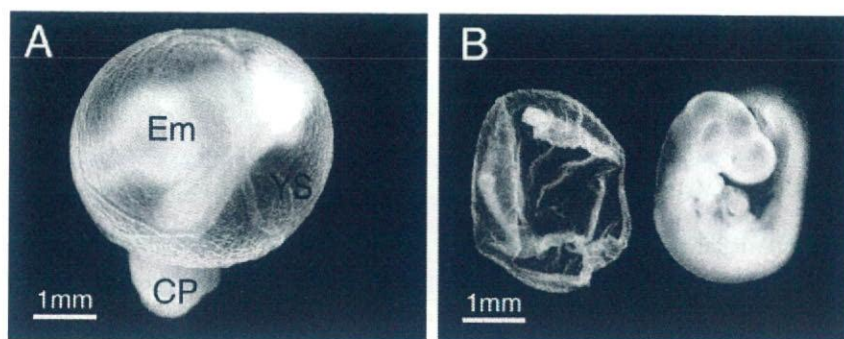
Fig. 1. Appearance of a rat embryo cultured for 24 h from day 10.5 of gestation: (A) At the end of culture. Em, embryo; YS, yolk sac; CP, chorio-allantoic placenta. (B) After the separation of embryonic membranes. Left: yolk sac membrane, Right: embryo.

single gel. The protein spots were identified by mass spectrometry for the construction of a primary 2-DE map of cultured postimplantation rat embryos. The same method could be applied to the 2-DE analysis of yolk sac membranes.

2. Materials and methods

2.1. Embryo culture

Rat embryos were cultured for 24 h by the roller bottle method as previously described (Usami and Ohno, 1996). Embryos were explanted from pregnant Wistar rats (Crlj: WI, Charles River Laboratories Japan, Inc., Kanagawa, Japan) at day 10.5 of gestation (plug day = day 0.5) under ether anesthesia. Explanted embryos were placed in a culture bottle at one embryo per 0.8–1 ml of rat serum and rotated at 35 rpm for 24 h at 37–38 °C. After the culture, the embryos and yolk sac membranes were washed three times with ice-cold buffer (0.01 M Tris–HCl, pH 7.0, 0.15 M NaCl), and placed in 1.5-ml eppendorf tubes individually with a minimum amount of the buffer for storage at −80 °C.

2.2. Preparation of embryo or yolk sac membrane samples

For 2-DE, frozen embryos or yolk sac membranes were lysed in 300 μl of rehydration buffer consisting of 7 M urea, 2 M thiourea, 2% (w/v) CHAPS, 2% (w/v) SB-10, 0.5% (v/v) IPG buffer (Amersham Biosciences, Piscataway, NJ) and 0.12% (v/v) DeStreak Reagent (Amersham Biosciences), by pulsed sonication with a 7-mm ∅ tip immediately after the addition of the buffer. Care was taken to avoid heating and forming during the sonication. Embryo or yolk sac membrane lysates were kept at 20 °C and their protein concentration was determined with the 2D Quant Kit (Amersham Biosciences).

2.3. Isoelectric focusing (IEF) for the first dimension of 2-DE

IEF was carried out on 13-cm immobilized pH gradient (IPG) strips (Immobiline DryStrip pH 3–10 NL, Amer-

sham Biosciences) with the IPGphor system (Amersham Biosciences). IPG strips were rehydrated with the rehydration buffer containing 50 μg protein of embryo or yolk sac membrane lysate for at least 12 h at 20 °C under a cover with silicon oil. Before the start of IEF, 3-mm-wide IEF electrode strips (Amersham Biosciences) damped were inserted between the IPG strip and both electrodes as electrode pads. Electrophoresis conditions were – Step 1: Step-n-hold at 500 V for 1 h, Step 2: Gradient at 1000 V for 1 h, Step 3: Gradient 8000 V for 2.5 h with the current limit of 50 μA per IPG strip. When electrophoresis for the second dimension was not carried out immediately after IEF, the IPG strips were stored at −80 °C.

2.4. Sodium dodecyl sulfate–polyacrylamide gel electrophoresis (SDS–PAGE) for the second dimension of 2-DE

SDS–PAGE was performed according to the method of Laemmli (Laemmli, 1970) except that no stacking gel was used. After IEF, IPG strips were equilibrated with 5 ml of SDS equilibration buffer consisting of 0.05 M Tris–HCl, pH 8.8, 6 M urea, 30% (v/v) glycerol, 2% (w/v) SDS, 0.025% (w/v) bromophenol blue. For the first equilibration, IPG strips were placed in a tube containing equilibration buffer with dithiothreitol (50 mg/5 ml) and rocked for 20 min. For the second equilibration, IPG strips were placed in a tube containing equilibration buffer with iodoacetamide (125 mg/5 ml) and rocked for 20 min. Equilibrated IPG strips were applied onto polyacrylamide gels (12.5% T, 2.6% C, 14 × 6 cm) and sealed with 0.5% agarose in electrode buffer. Electrophoresis was carried at a constant current of

Table 1
Size and protein content of cultured rat embryos

Item	Mean	Standard deviation
Yolk sac diameter (mm)	4.37	0.10
Crown-rump length (mm)	3.99	0.16
Number of somite pairs	26.0	0.67
Embryo protein (μg)	298.2	31.0
Yolk sac protein (μg)	153.0	20.2

Values for 10 embryos are shown.

10 mA per gel for 15 min and thereafter 20 mA per gel until the dye front reached the edge of the gel.

2.5. Stain of 2-DE gel and protein identification

After SDS–PAGE, 2-DE gels were stained with the Plus One Silver Staining Kit Protein (Amersham Biosciences) using the Multi Processor (Amersham Biosciences) according to the manufacturer's instruction. Stained 2-DE gels were scanned and analyzed with the PD Quest 2D analysis software (Bio-Rad, Hercules, CA).

For the identification of protein spots by mass spectrometry, 2-DE gels were stained with the mass-analysis compatible Proteo Silver staining kit (Sigma, St. Louis, MO) and protein spots were excised and cut into 1-mm cubes with a scalpel. Proteins in the gel cubes were digested with trypsin (Shevchenko et al., 1996), cleaned-up with Zip-Tip C18μ (Millipore, Bedford, MA) and analyzed by mass spectrometry using the 4700 Proteomics Analyzer (Applied Biosystems, Foster City, CA). The proteins were identified by the use of mass spectrometry data for the search of primary

sequence databases with the MS/MS ion search mode of the Mascot search engine (Matrix Science, Boston, MA).

3. Results

3.1. Embryo culture

Fig. 1A shows a cultured rat embryo at the end of the 24-h culture period. Embryos and yolk sac membranes were separated as samples for 2-DE analysis (Fig. 1B). The amnion and chorio-allantoic placenta were removed and discarded. The size and protein content of the embryos and yolk sac membranes of the cultured rat embryos are shown in Table 1. Protein content in the individual embryo or yolk sac membrane was sufficient for 2-DE anaylsis.

3.2. 2-DE of embryo protein

Proteins of cultured embryos were well separated by 2-DE with the present method (Fig. 2). About 800 protein spots were consistently detected in replicate gels each

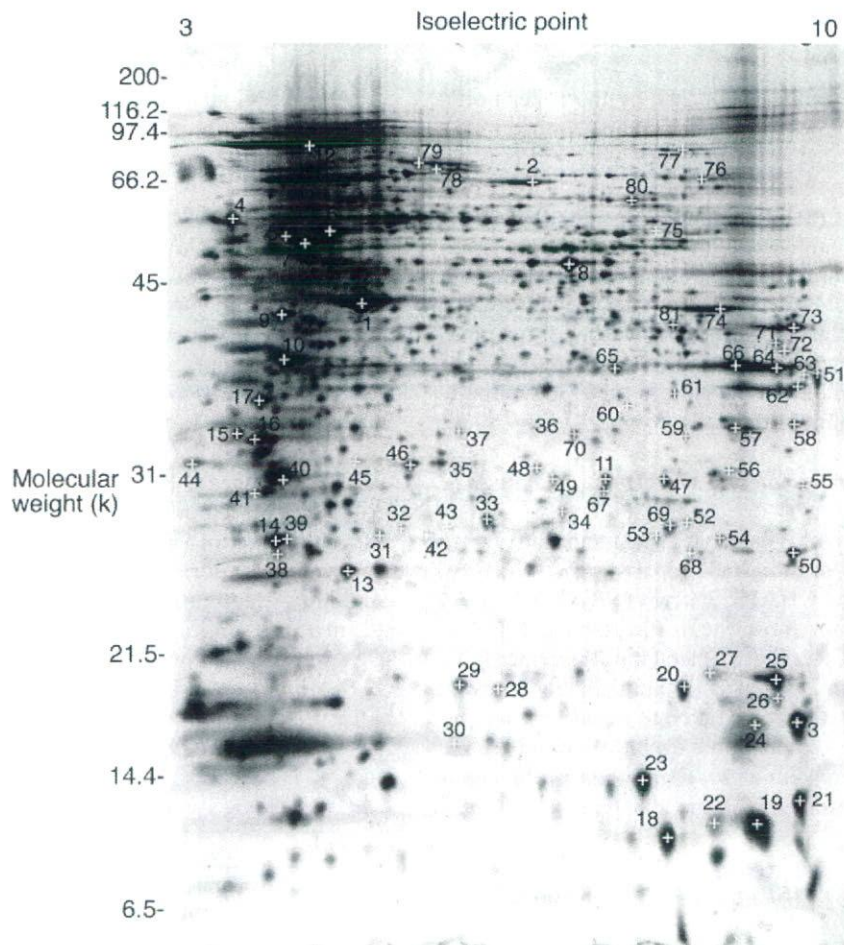Fig. 2. 2-DE pattern of embryo proteins from a cultured rat embryo equivalent to day 11.5 of gestation. Proteins (50 μg) were separated by IEF with 3–10NL IPG strip (13 cm) and by SDS–PAGE with 12.5% gel (14 × 6 cm), and were stained with silver. Identified protein spots were numbered and listed in Table 2.

Table 2
Protein spots identified in the 2-DE of embryo protein

Spot no.	Accession no.	Protein name	Nominal mass	Calculated pI
1	gi 71620	Actin beta	42,066	5.29
2	gi 19705431	Albumin	70,670	6.09
3	gi 37748460	Peptidylprolyl isomerase A	18,091	8.34
4	gi 11693172	Calreticulin	48,137	4.33
5	gi 202549	Iodothyronine 5′ monodeiodinase	54,375	4.87
6	gi 38014578	Tubulin, beta, 2	50,225	4.79
7	gi 54792127	ATP synthase, H$^+$ transporting, mitochondrial F1 complex, beta subunit	56,318	5.19
8	gi 38649320	Eno1 protein	51,736	6.70
9	gi 38014840	Laminin receptor 1	32,917	4.80
10	gi 112077	Nucleolar phosphoprotein B23.1	32,711	4.62
11	gi 12844989	Unnamed protein product	28,799	6.67
12	gi 51859516	Heat shock 90 kDa protein 1, beta	83,631	4.97
13	gi 8394432	Peroxiredoxin 2	21,941	5.34
14	gi 6678437	Tumor protein, translationally-controlled 1	19,564	4.76
15	gi 48675371	Complement component 1, q subcomponent binding protein	31,320	4.77
16	gi 34876714	Predicted: similar to Eukaryotic translation elongation factor 1 beta 2	24,831	4.55
17	gi 7242171	Proliferating cell nuclear antigen	29,108	4.66
18	gi 27668426	Predicted: similar to hemoglobin: Subunit = zeta	16,124	6.75
19	gi 3367724	Epsilon 1 globin	16,151	7.90
20	gi 55926145	Expressed in non-metastatic cells 2	17,386	6.92
21	gi 1628436	Profilin	15,149	8.46
22	gi 3367724	Epsilon 1 globin	16,151	7.90
23	gi 40254577	Ribosomal protein S12	14,905	6.81
24	gi 37748460	Peptidylprolyl isomerase A	18,091	8.34
25	gi 509201	Cofilin	18,749	8.22
26	gi 7441446	Destrin	18,661	7.78
27	gi 6671746	Cofilin 2, muscle	18,812	7.66
28	gi 19924089	Expressed in non-metastatic cells 1, protein (NM23A) (nucleoside diphosphate kinase)	17,296	5.96
29	gi 38328242	Stmn1 protein	17,278	5.76
30	gi 12850597	Unnamed protein product	17,138	5.95
31	gi 57006	Unnamed protein product	22,320	5.55
32	gi 202945	Apolipoprotein A-I precursor	30,100	5.52
33	gi 3688521	Thiol-specific antioxidant protein	24,860	5.64
34	gi 8394082	Proteasome (prosome, macropain) subunit, beta type 3	23,235	6.15
35	gi 20071222	NADH dehydrogenase (ubiquinone) Fe-S protein 3	30,358	6.40
36	gi 1381643	Cysteine protease p32-beta	30,097	5.68
37	gi 30410794	Proteasome activator subunit 3 isoform 1	29,602	5.69
38	gi 21312044	Eukaryotic translation initiation factor 3, subunit 12	25,356	4.81
39	gi 6671696	Chromobox homolog 1 (Drosophila HP1 beta)	21,519	4.85
40	gi 27664664	Predicted: similar to 25 kda FK506-binding protein	25,220	9.29
41	gi 6381991	Integrin beta 4 binding protein	27,007	4.63
42	gi 202945	Apolipoprotein A-I precursor	30,100	5.52
43	gi 2897818	Huntingtin interacting protein-2	22,503	5.33
44	gi 6978499	Acidic (leucine-rich) nuclear phosphoprotein 32 family, member A	28,718	3.99
45	gi 47169488	TPA: proteasome subunit alpha type 3-like	28,621	5.19
46	gi 62664759	Predicted: prohibitin	27,757	5.44
47	gi 297111	Phosphoglyceromutase	28,908	8.85
48	gi 16758298	Proteasome (prosome, macropain) subunit, beta type 7	30,250	8.13
49	gi 16758848	Endoplasmic retuclum protein 29	28,614	6.23
50	gi 56789700	Peroxiredoxin 1	22,323	8.27
51	gi 38648863	Malate dehydrogenase, mitochondrial	36,117	8.93
52	gi 16758182	RAN, member RAS oncogene family	24,579	7.01
53	gi 5420030	Glutathione transferase	25,550	6.77
54	gi 25453420	Glutathione S-transferase, pi	23,652	6.89
55	gi 56550075	Proteasome (prosome, macropain) subunit, alpha type 7	28,010	8.60
56	gi 8394069	Proteasome (prosome, macropain) subunit, alpha type 4	29,764	7.59
57	gi 18543331	Guanine nucleotide binding protein, beta polypeptide 2-like 1	35,529	7.60
58	gi 38051979	Vdac1 protein	32,060	8.35
59	gi 1906812	Inducible carbonyl reductase	30,920	7.64
60	gi 62661724	Predicted: similar to esterase D/formylglutathione hydrolase	37,322	6.45

Table 2 (continued)

Spot no.	Accession no.	Protein name	Nominal mass	Calculated pI
61	gi 57527447	Ribose-phosphate pyrophosphokinase I -like	35,297	6.51
62	gi 54261548	Lactate dehydrogenase A	36,712	8.45
63	gi 7949053	Heterogeneous nuclear ribonucleoprotein A2/B1 isoform 1	36,028	8.67
64	gi 62653546	Predicted: similar to glyceraldehyde-3-phosphate dehydrogenase	36,045	8.44
65	gi 6978491	Aldehyde reductase 1	36,230	6.26
66	gi 62653546	Predicted: similar to glyceraldehyde-3-phosphate dehydrogenase	36,045	8.44
67	gi 76647405	Predicted: similar to proteasome subunit alpha type 6 (proteasome iota chain) (macropain iota chain)	27,838	6.34
68	gi 8394079	Proteasome (prosome, macropain) subunit, beta type 2	23,069	6.96
69	gi 8394063	Proteasome (prosome, macropain) subunit, alpha type 2	26,024	6.92
70	gi 62655706	Predicted: similar to RIKEN cdna 1110025F24	26,482	5.90
71	gi 61889115	Phosphoserine aminotransferase 1	40,943	7.57
72	gi 66911068	Pcbp2_predicted protein	35,666	8.17
73	gi 202837	Aldolase A	39,691	8.31
74	gi 38649310	Phosphoglycerate kinase 1	44,909	8.02
75	gi 584875	Adenylyl cyclase-associated protein 1 (CAP 1)	51,857	7.16
76	gi 74144333	Unnamed protein product	67,573	7.18
77	gi 19424312	KH-type splicing regulatory protein	74,466	6.38
78	gi 228784	Alpha fetoprotein	70,167	5.71
79	gi 228784	Alpha fetoprotein	70,167	5.71
80	gi 2511703	p60 protein	63,158	6.40
81	gi 2644966	hnRNP-E1 protein	37,987	6.66

Proteins names with their NCBI accession numbers were shown for the protein spots in Fig. 1.

from one embryo. Selected protein spots were analyzed by mass spectrometry and 81 protein spots were identified as shown in Table 2. These protein spots also served as landmarks for the matching of protein spots among the gels.

3.3. 2-DE of yolk sac membrane protein

Proteins of yolk sac membranes were separated as well as those of embryos by 2-DE with the present method (Fig. 3). The 2-DE pattern of yolk sac membranes was fairly different from that of embryos. Most protein spots were common but were quantitatively different between the yolk sac membranes and the embryos. In addition, there were embryo specific and yolk sac membrane specific protein spots.

4. Discussion

The present method is simple and can be carried out concomitantly with in vitro developmental toxicity studies using rat embryo culture. The whole 2-DE procedures are completed within four days. IPG strips with narrower pH ranges would be useful for precise and convenient analysis of specific protein spots. For screening purposes or focused proteomics, the same procedures could be applied to the mini-gel format with shorter IPG strip and mini SDS–PAGE gel.

The primary 2-DE map constructed in the present study is useful for interlaboratory comparison of 2-DE patterns. Abundant and characteristic protein spots can be used as landmarks for matching of the 2-DE pattern. We are planning to identify more protein spots for a more precise and

accurate 2-DE map of cultured rat embryos in future, giving priority to protein spots of interest that are differentially expressed due to the effects of developmental toxicants. Identification of very faint protein spots may require a separate 2-DE experiment with an increased amount of applied protein samples.

It is expected that 2-DE analysis by the present method enables informative experiments for developmental toxicity studies. Because protein from less than one embryo is sufficient for 2-DE analysis in the present method, toxic effects observed in individual embryos may be related to the changes in protein expression pattern. Alternatively, analysis of specific parts isolated from single embryos may improve the efficiency of differential analysis. It is also noted that the present method is valid for 2-DE analysis of yolk sac membranes as well as embryos. Simultaneous analysis of yolk sac membranes with embryos would be useful to investigate the action sites of developmental toxicants.

The critical point of the present method is the use of the DeStreak Reagent as an antioxidant and the electrode pads. Both of which greatly improved the 2-DE pattern by decreasing horizontal streaks in the present method. We initially used dithiothreitol or tributylphosphine as a reducing agent to avoid the oxidation of proteins but could not decrease the streaks sufficiently. High concentration of redox agents such as glutathione in the embryo or yolk sac membrane samples (Harris et al., 1995) might affect redox status of proteins when dithiothreitol or tributylphosphine was used.

As far as we tested, addition of protease inhibitors to the lysis/rehydration buffer had no effects on the 2-DE pattern. It is considered that the constituents of the lysis/rehydration buffer were effective for inactivation of proteases in the
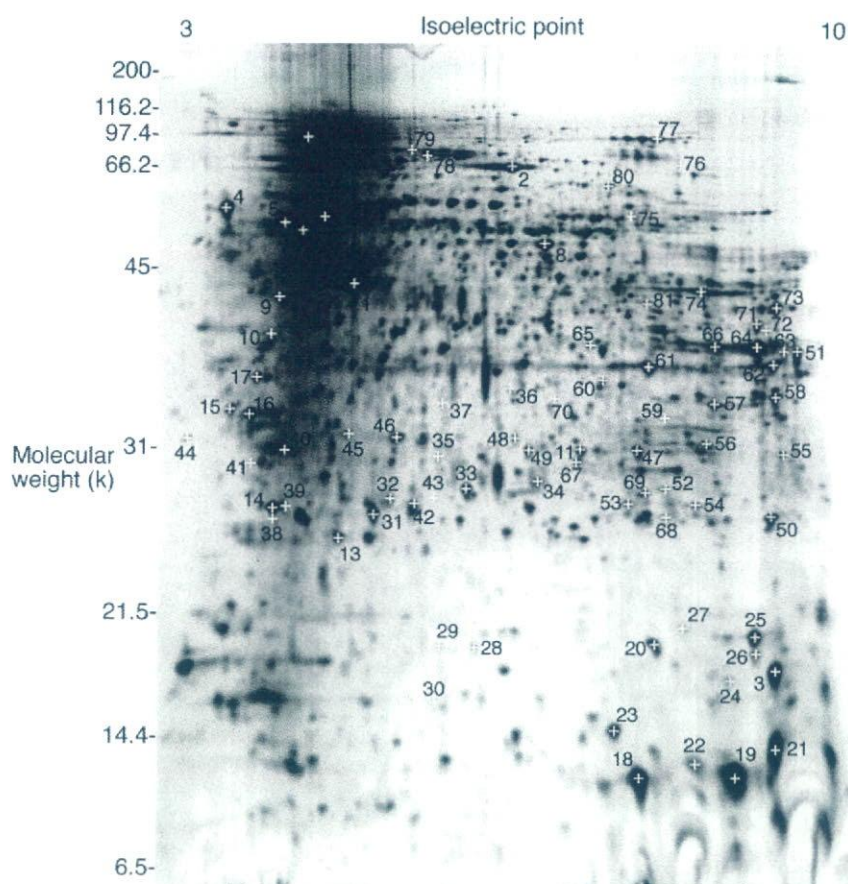
Fig. 3. 2-DE pattern of yolk sac membrane proteins from a cultured rat embryo equivalent to day 11.5 of gestation. Proteins (50 μg) were separated by IEF with 3–10NL IPG strip (13 cm) and by SDS–PAGE with 12.5% gel (14 × 6 cm), and were stained with silver. Proteins identified for the embryo are indicated by the same number as in Fig. 2.

embryo or yolk sac membrane samples. No requirement for protease inhibitors in the present method saves the const and labor in the 2-DE analysis.

In conclusion, it is considered that the present method is suitable for 2-DE analysis of embryos and yolk sac membranes in developmental toxicity studies using postimlantation rat embryo culture.

Acknowledgements

References

Baumgartner, B.G., Murach, K.-F., Schlegel, E., Praxmayer, C., Illmensee, K., 1994. Comparison of protein analysis between embryonic and extraembryonic tissues during the 11th day of gestation of the mouse. Electrophoresis 15, 992–1000.

Fountoulakis, M., Berndt, P., Boelsterli, U.A., Crameri, F., Winter, M., Albertini, S., Suter, L., 2000. Two-dimensional database of mouse liver proteins: Changes in hepatic protein levels following treatment with acetaminophen or its nontoxic regioisomer 3-acetamidophenol. Electrophoresis 21, 2148–2161.

Greene, N.D.E., Leung, K.-Y., Wait, R., Begum, S., Dunn, M.J., Copp, A.J., 2002. Differential protein expression at the stage of neural tube closure in the mouse embryo. J. Biol. Chem. 277, 41645–41651.

Harris, C., Hiranruengchok, R., Lee, E., Berberian, R.M., Eurich, G.E., 1995. Glutathione status in chemical embryotoxicity: Synthesis, turnover and adduct formation. Toxicol. in Vitro 9, 623–631.

Laemmli, U.K., 1970. Cleavage of structural proteins during the assembly of the head of bacteriophage T4. Nature 227, 680–685.

Piubelli, C., Cecconi, D., Astner, H., Caldara, F., Tessari, M., Carboni, L., Hamdan, M., Righetti, P.G., Domenici, E., 2005. Proteomic changes in rat serum, polymorphonuclear and mononuclear leukocytes after chronic nicotine administration. Proteomics 5, 1382–1394.

Praxmayer, C., Murach, K.-F., Baumgartner, B., Aberger, F., Schlegel, E., Illmensee, K., 1992. Protein synthesis in murine organs during postimplantation development detected by two-dimensional gel electrophoresis. Electrophoresis 13, 720–722.

Schmid, B., Bechter, R., Kucera, P., 1997. Use of whole emryo cultures in in vitro teratogenicity testing. In: Castell, J.V., Gómez-Lechón, M.J. (Eds.), In Vitro Methods in Pharmacetical Research. Academic Press, San Diego, pp. 353–373.

Shevchenko, A., Wilm, M., Vorm, O., Mann, M., 1996. Mass spectrometric sequencing of proteins from silver-stained polyacrylamide gels. Anal. Chem. 68, 850–858.

Usami, M., Ohno, Y., 1996. Teratogenic effects of selenium compounds on cultured postimplantation rat embryos. Teratog. Carcinog. Mutagen. 16, 27–36.

Xu, H., Hu, L.S., Chang, M., Jing, L., Zhang, X.Y., Li, G.S., 2005. Proteomic analysis of kidney in fluoride-treated rat. Toxicol. Lett. 160, 69–75.

Short communication

Fetal cartilage malformation by intravenous administration of indium trichloride to pregnant rats

Mikio Nakajima [a], Hiroki Takahashi [a], Ken Nakazawa [b], Makoto Usami [b],*

[a] *Pharmaceuticals R and D Division, Asahi Kasei Pharma Corporation, Japan*
[b] *Division of Pharmacology, National Institute of Health Sciences, 1-18-1, Kamiyoga, Setagaya, Tokyo 158-8501, Japan*

Abstract

The effects of indium on bone and cartilage development in rat fetuses were examined. Pregnant Sprague Dawley (SD) rats were treated with indium trichloride (0.1, 0.2, or 0.3 mg/kg) by single intravenous administration on Day 10 of gestation, and their fetuses were examined on Day 21. Half of each litter was prepared for skeletal examinations using a skeletal double-staining technique to allow evaluation of cartilage as well as bone. Dose-related increased incidences of external and skeletal fetal malformations occurred at doses of 0.2 mg/kg or more. The incidences of cartilage malformations in the vertebrae, ribs, and forepaw phalanges were significantly increased at 0.3 mg/kg. Malformations of the axial bone were accompanied by cartilage malformations. It was concluded from these results that indium produced cartilage malformations, that were considered to be the underlying cause for the majority of fetal skeletal malformations observed in rats in this study.
© 2007 Elsevier Inc. All rights reserved.

Keywords: Cartilage; Bone; Skeleton; Fetus; Malformation; Indium trichloride; Sprague Dawley rat; Teratogenicity

1. Introduction

Indium, a metal commonly used for semiconductors in industry and for scintigraphy in medicine, is teratogenic in rats. Single intravenous administration of indium trichloride (0.4 mg/kg) to pregnant rats on Days 8, 9, or 10 of gestation caused external, skeletal, and visceral malformations in the fetuses [1,2]. Brachyury, anury, kinked tail, anal atresia, and oligodactyly were observed as external malformations. Undesdended testis and dilatation of renal pelvis were observed as visceral malformations. Skeletal malformations were observed in the vertebrae, ribs, and sternebrae.

Indium may also affect cartilage development in the fetuses since the axial skeleton is formed by replacement of the cartilage by bone [3]. Potential cartilage malformations produced by indium, however, have not been reported, since fetal specimens in previous studies were examined following staining only for ossified bones using alizarin red S. Therefore in the present study, we extended the examination of indium teratogenicity in rats by using a double-staining method, which allowed an assessment of both fetal bone and cartilage development in rat fetuses.

2. Materials and methods

2.1. Animals and administration of indium

Pregnant Sprague Dawley (SD) rats (Crl: CD (SD), 9–11 week's old, weighing 240–280 g, Charles River laboratories Japan, Inc., Kanagawa, Japan) at Days 5 or 6 of gestation (sperm positive vaginal smear, Day 0) were purchased from Charles River Japan, Inc. (Kanagawa, Japan). They were housed as previously described [1]. Indium trichloride (InCl$_3$·4H$_2$O, Wako pure chemical industry Ltd., Osaka, Japan) dissolved in physiological saline was injected into a tail vein of the pregnant rats on Day 10 of gestation. Pregnant rats in the control group were given physiological saline at 1 ml/kg in the same manner. Forty rats were divided into four groups (10 per group) and of which 8 (control), 10 (0.1 mg/kg), 9 (0.2 mg/kg), and 10 (0.3 mg/kg) rats were confirmed as pregnant at term.

2.2. Observation and examination

Clinical observation of the animals was made daily. Body weight was measured on Days 6, 8, 10, 12, 14, 16, 18, and 21 of gestation. Body weight gain was

---

calculated for each interval between the body weight measurements. The pregnant rats were sacrificed on Day 21 of gestation by exsanguination under ether anesthesia. The gravid uterine horns were removed and the numbers of dead implants and live fetuses were counted. Live fetuses were sexed, weighed individually, and examined for external malformations. The placentas were weighed individually. All live fetuses were examined for potential skeletal malformations after standard KOH clearing and staining. Half of the fetuses from each litter was double stained with alizarin red S and alcian blue 8GS for assessment of bone and cartilage [4]. The remaining half of the fetuses from each litter was stained only with alizarin red S [5] as in a previous study [1]. No visceral examination of the fetuses was made in the present study.

2.3. Statistical analysis

A pregnant animal or a litter was used as a sample unit, and statistical significance of differences between the control and indium groups was examined at 5 and 1% probability levels. Fisher's exact test was used for categorical data. One-way analysis of variance was used for parametric data with homogeneous variance among the groups as determined by Bartlett test. Kruskal–Wallis H test was used for parametric data without homogenous variance and for nonparametric data. When the results of these parametric or nonparametric analysis of variance were significant at a 5% probability level, comparisons were made between the control and indium groups by parametric or nonparametric Dunnett's test using SAS Version 6.12 incorporated in a toxicology study-supporting system TOXstaff21 (CTC laboratory systems corp., Tokyo, Japan).

3. Results

No obvious toxicological signs and necropsy findings were observed in the pregnant rats in any experimental groups. There were no significant differences in the body weight of pregnant rats between the control and indium treatment groups, although reduced body weight gains were observed after the administration of indium on Days 14, 18, and 21 of gestation at 0.3 mg/kg and on Day 14 at 0.2 mg/kg probably due to the increased mortality of implants and the decreased fetal weights (Fig. 1). Table 1 shows fetal growth on Day 21 of gestation in pregnant rats treated with indium. There were no significant differences at 0.1 and 0.2 mg/kg. Mortality of implants was significantly increased at 0.3 mg/kg. There were dose-related decreases in fetal weight with remarkable significant decreases at 0.3 mg/kg in both male and female fetuses. Placental weight was significantly decreased at 0.3 mg/kg in female fetuses.
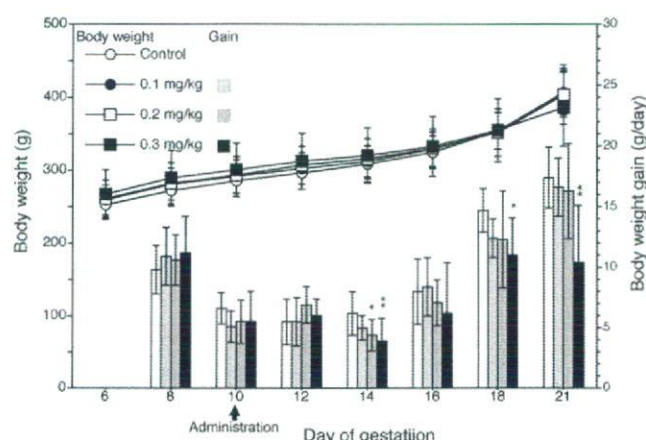

Fig. 1. Body weight and body weight gain of pregnant rats treated with indium trichloride on Day 10 of gestation. Vertical bars represent S.D. Asterisks indicate significant differences compared with the control group (*, $p < 0.05$, **, $p < 0.01$).

External malformations observed in the fetuses are shown in Table 2. There were significant increases in the incidence of external malformations at 0.2 and 0.3 mg/kg. Malformations of caudal part, that is, brachyury, anury, kinked tail, anal atresia, and of digits were observed at high incidences. The incidence of kinked tail at 0.2 mg/kg was higher than that at 0.3 mg/kg in contrast to the increased incidences of anury and brachyury at 0.3 mg/kg, suggesting that the kinked tail was a moderate manifestation of tail malformations by indium.

Skeletal abnormalities observed in alizarin red S-stained fetal specimens are shown in Table 3. There were significant increases in the incidence of skeletal malformations at 0.2 and 0.3 mg/kg. It was noted that malformations of the axial skeleton, that is, the vertebrae, ribs, and sternebrae were observed at high incidences. Malformations of the forelimb were also observed at high incidences at 0.3 mg/kg.

Skeletal abnormalities observed in double-stained fetal specimens are shown in Table 4. The incidences of cartilage malformations in the vertebrae, ribs, and forepaw phalanges were significantly increased at 0.3 mg/kg. Severe cartilage mal-

Table 1
Fetal growth in pregnant rats treated with indium trichloride

	Dose (mg/kg)			
	0 (Control)	0.1	0.2	0.3
No. of pregnant rats	8	10	9	10
No. of implants[a]	13.3 ± 1.3	13.6 ± 2.1	13.6 ± 1.9	14.6 ± 2.8
Mortality of implants (%)	1.0	4.5	3.3	31.3**
No. of live fetuses[a]	13.1 ± 1.5	13.0 ± 2.3	13.1 ± 1.8	10.1 ± 4.4
Sex ratio (M/M + F)	0.49	0.52	0.46	0.48
Fetal weight (g)[a]				
Male	5.73 ± 0.43	5.46 ± 0.44	5.33 ± 0.32	3.76 ± 1.16**
Female	5.48 ± 0.28	5.21 ± 0.48	5.05 ± 0.27	3.47 ± 0.95**
Placental weight (g)[a]				
Male	0.45 ± 0.05	0.45 ± 0.04	0.45 ± 0.04	0.38 ± 0.13
Female	0.45 ± 0.06	0.45 ± 0.06	0.44 ± 0.07	0.35 ± 0.11*

[a] Means ± S.D. are shown. Asterisks indicate significant differences compared with the control group (*, $p < 0.05$; **, $p < 0.01$).

Table 2
External malformation in the fetuses of pregnant rats treated with indium trichloride

	Dose (mg/kg)			
	0 (Control)	0.1	0.2	0.3
No. of litters	8	10	9	10
No. of fetuses examined	105	130	118	101
No. of fetuses with external malformation	1 (0.8%)	0	48 (41.3%)	93 (92.9%)**
Micrognathia	0	0	0	2 (2.4%)
Cleft palate	0	0	0	3 (2.3%)
Anal atresia	0	0	0	31 (38.5%)*
Anury	0	0	0	39 (43.0%)**
Kinked tail	0	0	47 (40.6%)*	32 (28.0%)
Brachyury	1 (0.8%)	0	38 (32.9%)	52 (48.1%)**
Short trunk	1 (0.8%)	0	0	1 (1.7%)
Small limb	0	0	0	43 (41.3%)**
Club foot	1 (0.8%)	0	0	26 (27.7%)
Oligodactyly	1 (0.8%)	0	3 (2.4%)	69 (72.6%)**
Distorted abdomen	0	0	0	7 (5.4%)

Asterisks indicate significant differences in the percentage incidence per litter compared with the control group (*, $p < 0.05$; **, $p < 0.01$). Numbers in parentheses are means of incidences per litter.

formations, such as fused, short, and absent ribs, were observed in unossified regions by the double staining (Fig. 2). There were increases in the incidence of malformations of the bone at 0.2 and 0.3 mg/kg as in specimens stained with alizarin red S alone, although no statistical significance was observed at 0.2 mg/kg. It was noted that the bone malformations were accompanied by the cartilage malformations, and that the incidences of rib malformations of the cartilage were higher than those of the bone.

As overall findings through the external, single-stained, and double-stained skeletal specimens, two or more malformations were observed in identical malformed fetuses, indicating multiple malformations at 0.2 and 0.3 mg/kg. Unexpectedly, the external tail malformations could not be related to malformed vertebrae of the tail, because consistent observation of the verte-

brae of malformed tails such as anury, kinked tail, and brachyury was difficult and the results were summarized with other regions as deformed vertebrae.

4. Discussion

It has been shown that double staining of fetal skeleton with alizarin red S and alcian blue 8GS is useful for skeletal examination in developmental toxicity studies [4]. In the present study, it was indicated that indium caused fetal cartilage malformations at high incidences when administered to pregnant rats on Day 10 of gestation. Severity and high incidences of cartilage malformations of the ribs indicate that observation of fetal cartilage is important for evaluation of effects of indium on fetal development. It is considered that the double-staining technique is also

Table 3
Skeletal abnormalities in alizarin red S-stained fetal specimens from pregnant rats treated with indium trichloride

	Dose (mg/kg)			
	0 (Control)	0.1	0.2	0.3
No. of litters	8	10	9	10
No. of fetuses examined	50	61	56	49
No. of fetuses with skeletal malformation	0	0	29 (54.1%)*	45 (91.3%)**
Deformed vertebra	0	0	29 (54.1%)*	44 (89.3%)**
Deformed rib	0	0	9 (17.0%)	38 (80.0%)**
Deformed sternebra	0	0	7 (13.9%)	37 (77.8%)**
Deformed scapula	0	0	0	4 (6.7%)
Absent ulna	0	0	0	25 (55.6%)**
Absent or deformed femur	0	0	0	4 (7.7%)
Absent tibia	0	0	0	3 (6.0%)
Deformed forepaw phalanx	0	0	0	32 (70.5%)**
No. of fetuses with skeletal variation	8 (16.5%)	5 (8.5%)	6 (11.2%)	2 (5.0%)
Cervical rib	0	0	3 (5.6%)	2 (5.0%)
Short supernumerary rib	8 (16.5%)	5 (8.5%)	3 (5.7%)	0

Asterisks indicate significant differences in the percentage incidence per litter compared with the control group (*, $p < 0.05$; **, $p < 0.01$). Numbers in parentheses are means of incidences per litter.

Table 4
Skeletal abnormalities in double-stained fetal specimens from pregnant rats treated with indium trichloride

	Dose (mg/kg)			
	0 (Control)	0.1	0.2	0.3
No. of litters	8	10	9	10
No. of fetuses examined	55	69	62	52
No. of fetuses with skeletal malformation	3 (5.1%)	8 (12.0%)	31 (53.7%)	51 (98.3%)**
Cartilage malformation	3 (5.1%)	8 (12.0%)	29 (49.5%)	51 (98.3%)**
Deformed vertebra	1 (1.6%)	0	6 (11.0%)	29 (62.1%)**
Deformed rib	3 (5.1%)	8 (12.0%)	25 (43.1%)	49 (95.6%)**
Absent metacarpal	0	0	0	2 (3.4%)
Deformed forepaw phalanx	1 (1.6%)	0	2 (3.4%)	37 (74.6%)**
Deformed hindpaw phalanx	1 (1.6%)	0	0	9 (23.1%)
Bone malformation	1 (1.6%)	0	30 (51.9%)	51 (98.3%)**
Deformed vertebra	1 (1.6%)	0	30 (51.9%)	50 (97.2%)**
Deformed rib	1 (1.6%)	0	4 (7.5%)	46 (89.7%)**
Deformed sternebra	0	0	8 (14.7%)	42 (83.6%)**
Deformed scapula	0	0	0	9 (24.0%)*
Absent ulna	0	0	0	25 (55.2%)**
Absent or deformed femur	0	0	1 (2.2%)	11 (25.6%)**
Absent tibia	0	0	0	9 (22.5%)**
Deformed ilium	0	0	0	1 (1.4%)
Deformed forepaw phalanx	1 (1.6%)	0	2 (3.4%)	37 (74.6%)**
Deformed hindpaw phalanx	1 (1.6%)	0	0	9 (23.1%)
No. of fetuses with skeletal variation	9 (16.2%)	7 (9.5%)	6 (9.2%)	6 (15.6%)
Cervical rib	0	1 (1.3%)	1 (1.6%)	2 (7.0%)
Short supernumerary rib	9 (16.2%)	6 (8.2%)	5 (7.6%)	4 (8.6%)

Asterisks indicate significant differences in the percentage incidence per litter compared with the control group (*, $p < 0.05$; **, $p < 0.01$). Numbers in parentheses are means of incidences per litter.

useful for the observation of effects of indium on both cartilage and bone, since malformations of the bone was observed equally as well as by single staining with alizarin red S.

The finding on the association of the bone malformations with the cartilage malformations may indicate that skeletal malformations following treatment with indium are due to abnormal development of the cartilage. This is because both the axial skeleton and limb bones, but not the skull, are entirely formed by ossification in the cartilage differentiated from mesoderm-derived cells [3,6]. It has also been reported
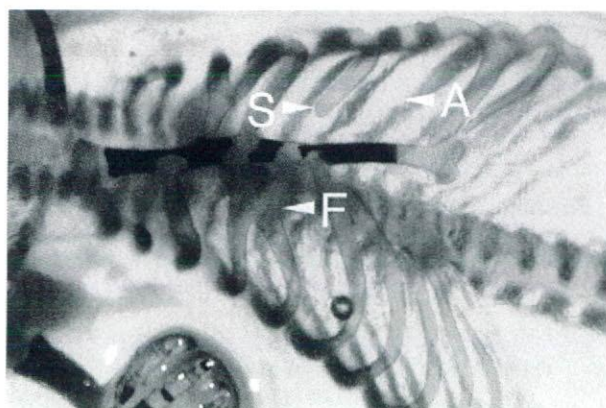

Fig. 2. Malformations of the rib cartilage in the fetuses of pregnant rats treated with indium trichloride. A ventral view of the thoracic region is shown with the head on the left side. A, absent rib; F, fused rib; S, short rib.

that indium disturbed the activity of chondrocytes; that is, oligosaccharides in femur chondrocytes of rat fetuses on Day 21 of gestation was decreased by oral administration of indium trichloride (400 mg/kg/day) to the dams through the gestation period [7].

In the present study, SD rats were used instead of Wistar rats because the present experiment was carried out as a part of joint group researches using SD rats. The major fetal malformations observed in SD rats have previously been observed in Wistar rats [1,2] including external malformations of the tail and limbs, and skeletal malformations of the vertebrae, ribs, and sternebrae. It is thus considered that there is no obvious strain difference between SD and Wistar rats in this respect.

In conclusion, these results suggest that indium produced cartilage malformations that may be the underlying cause for the majority of fetal skeletal malformations observed in rats in this study. Investigation of the cartilage malformations caused by indium is important for the evaluation of its effects on fetal development.

References

[1] Nakajima M, Takahashi H, Sasaki M, et al. Developmental toxicity of indium chloride by intravenous or oral administration in rats. Teratog Carcinog Mutagen 1998;18:231–8.
[2] Nakajima M, Takahashi H, Sasaki M, Kobayashi Y, Ohno Y, Usami M. Comparative developmental toxicity study of indium in rats and mice. Teratog Carcinog Mutagen 2000;20:219–27.

[3] Neubüser A, Balling R. Axial Skeleton. In: Kavlock RJ, Daston GP, editors. Drug toxicity in embryonic development I. Berlin: Springer; 1997. p. 77–112.

[4] Inouye M. Differential staining of cartilage and bone in fetal mouse skeleton by alcian blue and alizarin red S. Congenit Anom (Kyoto) 1976;16:171–3.

[5] Dawson AB. Note on the staining of the skeleton of cleared specimiens with alizarin red S. Stain Technol 1926;1:123–4.

[6] Brown NA. Nomal development: mechanisms of early embryogenesis. In: Kimmel CA, Buelke-Sam J, editors. Developmental toxicology. New York: Raven Press; 1994. p. 15–63.

[7] Ungváry G, Tátrai E, Szakmáry E, Náray M. The effect of prenatal indium chloride exposure on chondrogenic ossification. J Toxicol Environ Health A 2001;62:387–96.

Original Article

Comparative Proteome Analysis of the Embryo Proper and Yolk Sac Membrane of Day 11.5 Cultured Rat Embryos

Makoto Usami,[1*] Katsuyoshi Mitsunaga,[2] and Ken Nakazawa[1]

[1]Division of Pharmacology, National Institute of Health Sciences, Tokyo, Japan
[2]School of Pharmaceutical Sciences, Toho University, Chiba, Japan

BACKGROUND: Proteomic analysis of cultured postimplantation rat embryos is expected to be useful for investigation into embryonic development. Here we analyzed protein expression in cultured postimplantation rat embryos by two-dimensional electrophoresis (2-DE) and mass-spectrometric protein identification. **METHODS:** Rat embryos were cultured from day 9.5 for 48 h or from day 10.5 for 24 h. Proteins of the embryo proper and yolk sac membrane were isolated by 2-DE and differentially analyzed with a 2-D analysis software. Selected protein spots in the 2-DE gels were identified by matrix-assisted laser desorption/ionization-time of flight tandem mass spectrometric analysis and protein database search. **RESULTS:** About 800 and 1,000 protein spots were matched through the replicate 2-DE gels each from one embryo in the embryo proper and yolk sac membrane, respectively, and virtually the same protein spots were observed irrespective to the length of culture period. From protein spots specific to the embryo proper (126 spots) and yolk sac membrane (304 spots), proteins involved in tissue-characteristic functions, such as morphogenesis and nutritional transfer, were identified: calponin, cellular retinoic acid binding protein, cofilin, myosin, and stathmin in the embryo proper, and Ash-m, dimerization cofactor of hepatocyte nuclear factor, ERM-binding phosphoprotein, cathepsin, and legumain in the yolk sac membrane. **CONCLUSION:** Proteomic analysis of cultured postimplantation rat embryos will be a new approach in developmental biology and toxicology at the protein level. *Birth Defects Res (Part B)* 80:383–395, 2007. © 2007 Wiley-Liss, Inc.

Key words: *postimplantation embryo; development; 2-DE; MALDI-MS/MS; Wistar rat*

INTRODUCTION

Culture of postimplantation rat embryos has been widely used in the fields of developmental biology and toxicology, since it is considered that embryos can grow in vitro similarly to those in vivo during the culture period, which includes the early organogenetic period (Morriss-Kay, 1993). Usually, rat embryos at day 9.5 or 10.5 of gestation are cultured in rat serum for 24–48 h in roller bottles. There were no apparent differences other than slight growth retardation in the cultured embryos compared with the in vivo embryos although differences might be found by analysis using molecular techniques (Van Maele-Fabry et al., 1997; Williams et al., 1997).

Proteomic analysis of cultured postimplantation rat embryos is expected to be useful for investigation into embryonic development. Analysis of protein expression after experimental treatment of cultured embryos, such as exposure to chemicals, will reveal the proteins involved in normal or abnormal embryonic development. Application of antisense oligonucleotide or RNA interference techniques to the postimplantation embryo

culture (Calegari et al., 2002; Potts and Sadler, 1997) will support these proteomic experiments.

Recently, we established a two-dimensional electrophoresis (2-DE) method that enables analysis of individual cultured rat embryos (Usami et al., 2007). With this method, about 800 protein spots were isolated from the protein of cultured rat embryos equivalent to day 11.5 of gestation, and selected ones were identified by mass spectrometry. It was also shown that the yolk sac membrane has quantitatively and qualitatively different proteins compared to the embryo proper. It is thus expected that pairwise analyses of the individual embryo

WILEY InterScience®
DISCOVER SOMETHING GREAT

proper and yolk sac membrane provide intriguing information on the growth of postimplantation embryos.

In the present study, we examined 2-DE profiles of the embryo proper and yolk sac membrane of day 11.5 cultured rat embryos to further investigate their protein expression. Rat embryos at day 9.5 or 10.5 of gestation were cultured for 48 or 24 h, respectively, and proteins in the embryo proper and yolk sac membrane were isolated by 2-DE. The 2-DE profiles were compared between the varied length of culture periods and between the embryo proper and yolk sac membrane. Selected protein spots in the 2-DE gels were identified by mass spectrometry.

MATERIALS AND METHODS
Embryo Culture

Rat embryos were cultured by the roller bottle method as previously described (Usami and Ohno, 1996). Embryos were explanted from pregnant Wistar rats (Crlj: WI, Charles River Laboratories Japan, Inc., Kanagawa, Japan) at day 9.5 or 10.5 of gestation (plug day = day 0.5) under ether anesthesia. Explanted embryos were placed in a culture bottle at one embryo per 0.8–1 ml of rat serum and rotated at 35 rpm at 37–38°C. Day 9.5 embryos were cultured for 48 h and day 10.5 embryos for 24 h. After the culture, the embryos and yolk sac membranes were washed three times with ice-cold buffer (0.01 M Tris-HCl, pH 7.0, 0.15 M NaCl), and placed in 1.5-ml Eppendorf tubes individually with a minimum amount of the buffer for storage at −80°C.

2-DE Analysis

Proteins of the embryo proper and yolk sac membrane (50 μg/gel) were analyzed by 2-DE as previously described (Usami et al., 2007). IPG strips (Immobiline DryStrip pH 3–10NL, 13 cm, Amersham Biosciences, Piscataway, NJ) were used in IEF for the first dimension, and 12.5% polyacrylamide gels (14 × 16 cm) were used in SDS-PAGE for the second dimension. 2-DE gels were stained with Plus One Silver Staining Kit Protein (Amersham Biosciences) using Multi Processor (Amersham Biosciences). The stained 2-DE gels were scanned with the GS-800 calibrated densitometer (Bio-Rad, Hercules, CA) and analyzed with the PD Quest 8.0 2-D analysis software (Bio-Rad). The gel images were normalized by the total density in gel image mode. Statistical significance of the quantitative differences between protein spots was examined by the t-test at 1% probability levels after log transformation.

MS Analysis

For the identification of protein spots by mass spectrometry, 2-DE gels were stained with mass-analysis compatible ProteoSilver staining kit (Sigma, St. Louis, MO) and protein spots were excised into column-shape pieces about 1-mm diameter. Proteins in the gel pieces were digested with trypsin (Shevchenko et al., 1996), cleaned-up with Zip-Tip C18μ (Millipore, Bedford, MA) and spotted on a matrix-assisted laser desorption/ionization (MALDI) target plate with 2 mg/ml of CHCA (Sigma) as a matrix. The MALDI-time of flight tandem mass spectrometry (MALDI-TOF/TOF) analysis was carried out with the 4700 Proteomics Analyzer (Applied Biosystems, Foster City, CA). MS spectra were obtained by 5,000 laser shots at an intensity of 4,500 with a mass range from 9,00–4,000 focused at 2,100. Angiotensin II (monoisotopic mass: 1,045.5423, Sigma) and ACTH fragment 18–39 (monoisotopic mass: 2,465.1989, Sigma) were used as standards for external calibration. From the each MS spectrum, 15 highest peaks, excluding those of trypsin, were used for MS/MS analysis. MS/MS spectra were obtained by 8,000–10,000 laser shots at intensity of 4,500 with a precursor mass window from −4 to +5 without CID gas, and were processed with default calibration.

Protein Identification

The proteins were identified by the use of mass spectrometry data for the search of the NCBInr protein database (Version 20061221; 4,318,227 sequences; 1,487,489,705 residues) with the MS/MS ion search mode of the Mascot search engine (Matrix Science, Boston, MA). Peak list files were created by using the PeakTo-Mascot software (Applied Biosystems) with settings for the MS/MS peak filter as follows: Mass range: 60, Precursor-: 20, Excluded Mass Range File: none, Peak density: Max 50 peaks per 200Da, Min S/N: 10, Min Area: 100, Max Peak/Precursor: 200. Created peak list files were subjected to the database search with settings as follows: Database: NCBInr, Taxonomy: Rodentia, Enzyme: Trypsin, Allow up to: 1 missed cleavage, Fixed modifications: Carbamidomethyl (C), Variable modifications: Oxidation (M), Peptide tol. ±:2Da, MS/MS tol. ±:0.8 Da, Peptide charge: 1+, Monoisotopic button: on, Data format: Mascot generic, Instrument: MALDI-TOF/TOF. Protein scores more than 42 were considered as significant hits. The protein identification data including the protein score, sequence coverage and peptide sequence are provided as supporting information.

RESULTS
Growth of Cultured Embryos and Their 2-DE Profiles

The growth of rat embryos in the 48 h culture was a little inferior to that in the 24 h culture as indicated by the shorter crown-rump length (Table 1, Fig. 1). However, there were no differences in the appearance and number of somite pairs of the embryos between the 48 and 24 h culture.

Table 1
Growth of Cultured Postimplantation Rat Embryos Equivalent to Day 11.5

	48 h culture from day 9.5	24 h culture from day 10.5
Number of embryos	14	15
Yolk sac diameter (mm)	4.41 ± 0.05	4.32 ± 0.07
Crown-rump length (mm)	3.71 ± 0.04	3.98 ± 0.06*
Number of somite pairs	26.2 ± 0.21	25.9 ± 0.24

Mean ± SEM is shown.
*Significant differences from the 48 h culture by the t-test ($P < 0.01$).
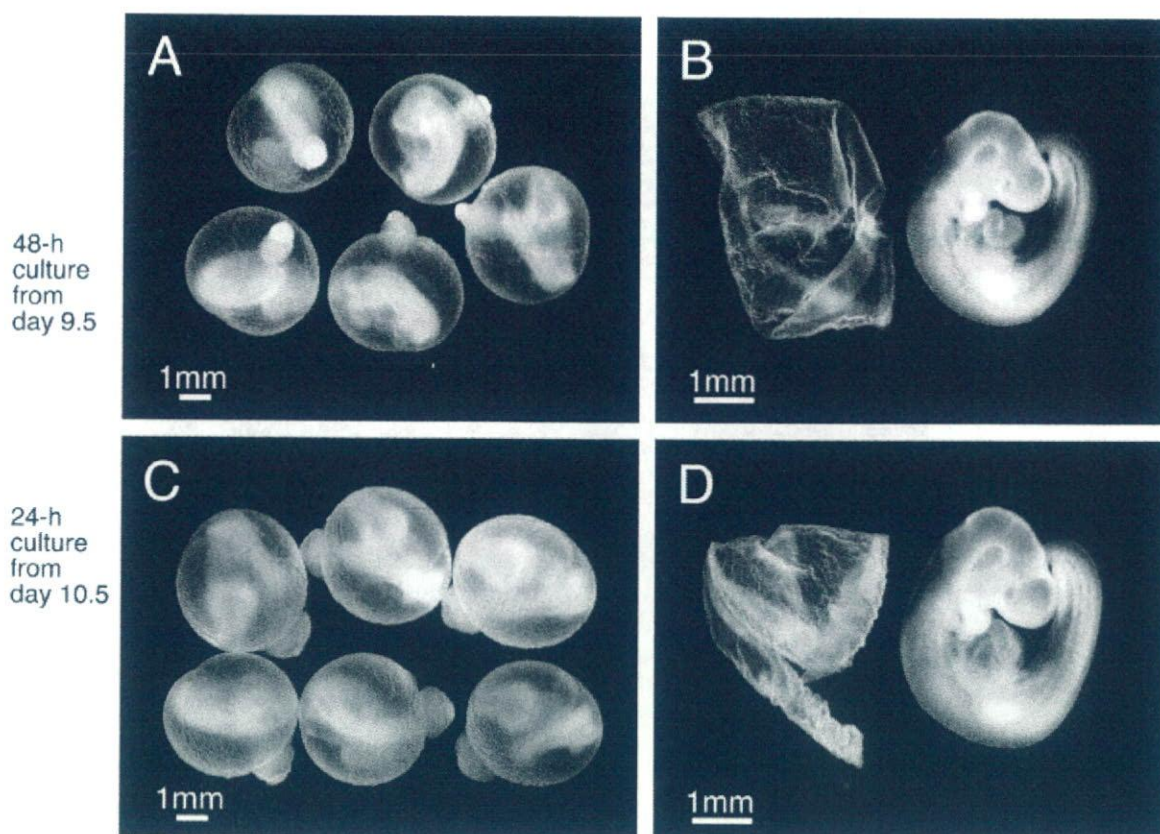
Fig. 1. Appearance of rat embryos equivalent to day 11.5 after 48 or 24 h culture from day 9.5 or 10.5. **A,C:** At the end of culture. **B,D:** After the separation of embryonic membranes. Left: yolk sac membrane; Right: embryo proper.

2-DE patterns of the embryo proper and yolk sac membrane of the cultured embryos are shown in Figs. 2 and 3. About 800 and 1,000 protein spots were matched through the replicate gels (5 gels for the 48 h culture and 6 gels for the 24 h culture) each from one embryo in the embryo proper and yolk sac membrane, respectively.

Differences in 2-DE Profiles of Rat Embryos Between the 48 h and 24 h Culture

No obvious qualitative differences in 2-DE profiles were observed between the 48 and 24 h culture, i.e., virtually the same protein spots were observed in each of the embryo proper and yolk sac membrane irrespective of the length of culture period.

Quantitative differences in the 2-DE profiles by the varied length of culture period are summarized in Table 2, and relative quantity of the significantly different protein spots are shown in Figs. 4 and 5. There were no quantitative differences in most of the protein spots between the 48 and 24 h culture. It was noted, however, that the frequencies of protein spots with a larger quantity were in contrast between the embryo proper and yolk sac membrane; i.e., larger-quantity spots were fewer in the 48 h culture than in the 24 h culture for the embryo proper, and vice versa for the yolk sac membrane. There appeared no relationship between the quantities and differences of the protein spots.

Selected protein spots that were quantitatively different between the 48 and 24 h culture were identified by MS analysis (Tables 3 and 4). It was noted that the larger-quantity spots in the 24 h culture included some RNA-binding proteins (special spot numbers (SSPs) 4515, 7406, 7821, 8807) in the embryo proper and some constitutive enzymes (SSPs 4706, 6602, 9404) in the yolk sac membrane. On the other hand, the larger-quantity spots in the 48-h culture included serum proteins, i.e., albumin (SSP 5828), transferrin (SSP 7807), and complement component 3 (SSPs 1010, 1017, 2018, 2108, 3006, 4105, 5111, 8009), in the yolk sac membranes.

Differences in 2-DE Profiles Between the Embryo Proper and Yolk Sac Membrane

Protein spots specific to either the embryo proper (126 spots) or yolk sac membrane (304 spots) are shown in Figs. 2 and 3. Of these specific spots, proteins identified so far are shown in Tables 5 and 6. Both embryo proper and yolk sac membrane had various specific protein spots, such as enzymes, translation factors, cytoskeletons, transporters, chaperons, and receptors. These included